Available online at www.sciencedirect.com
SCIENCE DIRECT®
Biochemical Pharmacology 67 (2004) 1499–1511
Biochemical Pharmacology
www.elsevier.com/locate/biochempharm

Nuclear factor Y regulation and promoter transactivation of human ribonucleotide reductase subunit M2 gene in a Gemcitabine resistant KB clone

Xiyong Liu[a], Bingsen Zhou[a], Lijun Xue[a], Weihua Qiu[a], Jennifer Shih[a], Shu Zheng[b], Yun Yen[a,*]

[a]*Department of Medical Oncology & Therapeutic Research, City of Hope National Medical Center, 1500 E. Duarte Road, Duarte, CA 91010-3000, USA*
[b]*Cancer Institute of Zhejiang University, 88 Jiefang Road, Hangzhou 310009, China*

Received 31 July 2003; accepted 15 December 2003

Abstract

Overexpression of human ribonucleotide reductase subunit M2 (*hRRM2*) has been shown as a potential factor causing Gemcitabine (Gem) resistance. We hypothesized the nuclear factor Y (NF-Y) would transcriptionally regulate *hRRM2* and contribute to overexpression of *hRRM2* in a Gem resistant clone. A luciferase and gel shift assay, and a Southwestern blot were employed to analyze the promoter activity of *hRRM2*. The data exhibited the *hRRM2* promoter was upregulated almost 5-fold in the Gem resistant KB clone (KBGem) via three sequential CCAAT boxes located in the proximal promoter region. Nuclear extracts from KB and KBGem could interact with the CCAAT motif of the *hRRM2* proximal promoter region, and could form DNA–protein complexes with different binding patterns. The complexes could be further recognized with antibodies against NF-Y subunits A and B. Histone deacetylases (HDAC) involvement in NF-Y transcription repression in the KBGem clone was examined. A HDAC activity assay revealed a 3-fold decrease of HDAC activity in the KBGem clone compared to KB cells. Parental cells were treated with trichostatin A (TSA), a HDAC inhibitor. NF-Y transactivation was induced, resulting in an increase of *hRRM2* expression. This led to an expanded dCTP pool and an abrogated [^{3}H]Gemcitabine incorporation. In addition, microarray analysis results showed most of the proliferation-related genes were upregulated in KBGem. This finding was consistent with enhanced NF-Y transactivation in KBGem. In summary, upregulation of NF-Y transactivation increased *hRRM2* transcription, which played a pivotal role in the Gem resistant KB clone.

Keywords: Ribonucleotide reductase; Promoter; Nuclear factor Y (NF-Y); CCAAT box; Drug resistance; Gemcitabine; Microarray

1. Introduction

Human ribonucleotide reductase is an important target for antineoplastic agents due to its key role in the synthesis of deoxyribonucleotides, which are necessary for DNA synthesis and repair. In eukaryotic cells, large α and small β subunits form an $\alpha_2\beta_2$ heterotetramer that is required for RR activity [1]. *hRRM2* and *p53R2* have been identified as two forms of the small subunit; *hRRM1* remains the only identified large subunit. The M1 subunit possesses a binding site for enzyme regulation and the M2 subunit contains a non-heme iron center and a tyrosyl free radical that is involved in RR activity [2]. The recently discovered *p53R2* subunit has been reported to be a *p53* dependent cell cycle checkpoint for DNA repair [3–5]. As with *hRRM2*, *p53R2* can interact with *hRRM1* to form an hRR complex that can supply resting cells with deoxyribonucleotides for DNA repair [6].

Gemcitabine, a nucleoside analogue, is important in the treatment of hematological malignancies and solid tumors. Gem is transported with an *hENT1* protein [7,8],

* Corresponding author. Tel.: +1-626-359-8111x62867; fax: +1-626-301-8233.
E-mail address: yyen@coh.org (Y. Yen).

Abbreviations: NF-Y, nuclear factor Y; hRR, human ribonucleotide reductase; *hRRM2*, human ribonucleotide reductase subunit M2; *hRRM1*, human ribonucleotide reductase subunit M1; p53R2, *p53* dependant ribonucleotide reductase subunit R2; KBGem, Gemcitabine drug resistance KB cell clone; HU, hydroxyurea; Gem, 2′,2′-dFdCyd[3], 2,2-difluorodeoxycytidine, Gemcitabine; TSA, trichostatin A; HDAC, histone deacetylases; HAT, histone acetyltransferases; hENT1, human equilibrative nucleoside transporter 1; DCK, deoxycytidine kinase; CDA, cytidine deaminase; 5′-Nucl, 5′-nucleotidase; dNTP, deoxynucleoside triphosphate; dCTP, deoxycytidine triphosphate.

0006-2952/$ – see front matter © 2004 Elsevier Inc. All rights reserved.
doi:10.1016/j.bcp.2003.12.026

phosphorylated by *DCK*, and then metabolized by several other enzymes to form dFdCDP and dFdCTP [9,10]. The phosphorylated Gem could be inactivated through dephosphorylation by *5′-Nucl* and further deaminated into its inactive form by *CDA* [7,11]. As a competitor of dCTP, dFdCTP is incorporated into DNA, causing masked chain termination [9,10]. On the other hand, Gem could act as the RR inhibitor and reduce dCTP, dATP, dGTP and dTTP pool sequentially [12]. Drug resistance is a major limitation of Gem in the treatment of cancer. The resistance could be caused by a number of factors affecting its metabolism, including *hENT1* deficiency [7,8], increased activity of nucleases that catalyzed the conversion of nucleotide back to nucleoside [11], loss of expression of *DCK* [13,14], and increased hRR activity [15]. Overexpression of hRR might expand the dNTP pool, which then competitively inhibits dFdCTP incorporation into DNA [9]. In addition, an expanded dNTP pool might limit Gem transportation and phosphorylation, and enhance the nucleotide deaminase to inactivate Gem into dFd-U via a negative feedback mechanism to prevent Gem incorporation. Our research group has selected a Gem resistant KB cell clone (KBGem) with stepwise exposure to Gem and demonstrated that overexpression of *hRRM2*—but not *hRRM1*—might play a primary role in Gem resistance [15]. We recently reported that the *hRRM2* gene could be detected in the Gem resistant KB clone arising in a homogeneous staining region (hsr) [16]. It was suggested that *hRRM2* gene amplification might be the source of increased transcription in KBGem cells. This finding could partly explain the increased expression of *hRRM2* in KBGem, but it is difficult to explain the overexpression of *hRRM2* without upregulation of the *hRRM2* promoter transactivation.

Promoter analysis results showed there were three CCAAT motifs within 140 base pairs upstream of the first transcription start site in the human *RRM2* subunit gene. Those three CCAAT boxes were found to contribute at least 50% of the maximal promoter activity and were responsible for cell-cycle specific expression [17,18]. Each CCAAT box seemed to contribute approximately 20–40% promoter activity in the proximal promoter region [18]. However, the genes for the human RR subunits *hRRM1* and *p53R2* were not reported to contain CCAAT-boxes. Several transcription factors, including CBF/NF-Y, CTF/NF-1 and C/EBP, have been isolated and reported binding to CCAAT motifs [19]. Among these, only CBF/NF-Y requires a high degree of conservation of the CCAAT sequence. The DNA consensus binding sequence of the other proteins often do not contain a complete CCAAT motif; only NF-Y has been distinguished as a CCAAT-binding protein on the basis of a requirement for this DNA sequence [19]. NF-Y is a heterotrimer composed of three subunits, *NF-YA* (*CBF-B*), *NF-YB* (*CBF-A*) and *NF-YC* (*CBF-C*). NF-Y subunits B and C form a histone fold that plays a crucial role in the creation of a functional NF-Y CCAAT box DNA binding complex; and NF-YA only interacts with the NF-YB:C heterodimer and not with NF-YB or NF-YC alone [20]. The histone-modifying enzymes, HAT and HDAC, have been reported to be involved in NF-Y transcription activation and repression, respectively [21].

In this study, we hypothesized NF-Y would interact with three sequential CCAAT boxes that are located in the *hRRM2* proximal promoter region, and transcriptionally regulate *hRRM2* expression; upregulation of NF-Y in KBGem clone would contribute to overexpression of *hRRM2* and play a pivotal role in Gem resistance.

2. Materials and methods

2.1. Cell culture, plasmids and transfection

The human oropharyngeal epidermal carcinoma cell line KB was purchased from the American Type Culture Collection (ATCC). Cells were grown in RPMI 1640 medium supplemented with 10% fetal bovine serum and 1% penicillin-streptomycin. A Gem resistant clone (KBGem) was selected and maintained in the presence of 8 μM Gem [15].

The reporter plasmid of pGL3 (Promega) was employed to construct a luciferase reporter gene for promoter activity analysis. The promoter fragments extending through position +1 and end points at positions −557, −455, −184, −106, −55, were generated to drive transcription of a luciferase gene as described previously [17] (Fig. 2B, left panel). The sequences of Pα, PB1, PB2, PB3, and PB4, corresponding to −61 to −152, −237 to −287, −357 to −397, −626 to −666 and −801 to −851 of the *hRRM2* promoter were inserted into the pGL3 vector to create luciferase reporter constructs. Pα is the wild-type sequence with three CCAAT motifs (5′-ggc aag gcg cag CCAAT ggg aag ggt cgg agg cat ggc aca g CCAAT ggg aag ggc cgg ggc acc aaa g CCAAT ggg aag ggc cgg gag c-3′), while PαMut1, PαMut12 and PαMut123 contained numbers 1, 2 and 3 of CCAAT boxes mutated to ACAAA (Fig. 2C, left panel). The insert DNA sequences of PB1 (5′-acg ggc cgg ggg ggg aac c GGGAG GTCCC ggg ggg cgt cca cgg ggg tgt-3′), PB2 (5′-cga acc ggg gcc cgc gcg CGCCA agg ccg ccg aga ccc tc-3′), PB3 (5′-tcc tcg ccg acc acc c CGCCA aaa tgt cag gcc tcg ggg c-3′) and PB4 (5′-gtt tac aaa gga ctg cac at TTTAC ATGAGTC atc tca acg aac gct ctc-3′) contained NF-κB (GGGAG and GTCCC), E2F (CGCCA), OCT-1 (TTTAC) and AP-1 (ATGAGTC) sites, respectively (Fig. 2C, left panel).

About 1–3 × 10^6 cells were suspended in 400 μL Eppendorf electroporation cuvettes (gap 2 mm) in hypoosmolar electroporation buffer and mixed with 10 μg test plasmid DNA and 5 μg pSV-β-galactosidase control plasmid (Promega). Electroporation was done for 75 μs at 800 V. After electroporation, cells were re-cultured for 48 hr and then harvested. Luciferase and β-galactosidase activities were detected using a Promega assay system. Promoter activation was determined based on relative

luciferase activity after normalizing to β-galactosidase activity to the control for varying transfection efficiency.

2.2. Gel shift and supershift assay

The sense and anti-sense strands of Pα12 (5′-ggc aag gcg cag CCA AT ggg aag g gtc gga ggc atg gca cag CCAAT ggg aag ggc cgg g-3′) and PαMut12 (CCAAT mutated to ACAAA) were synthesized by the City of Hope DNA Synthesis Facility. Annealed double stranded DNA fragments were labeled with [γ ^{32}P]ATP using T4 polynucleotide kinase.

DNA–protein binding reactions were performed in 4% glycerol, 1 mM $MgCl_2$, 0.5 mM EDTA, 0.5 mM DTT, 50 mM NaCl, 10 mM Tris–HCl (pH 7.5) and 0.05 mg/mL poly (dI-dC)·poly (dI-dC). Nuclear lysates (4 μg) and 0.035 pmol of [γ ^{32}P] end-labeled probe were incubated for 20 min at room temperature. For the supershift assay, 2 μg of NF-Y subunits A or B antibody (Santa Cruz) was included in the pre-incubation mixture. DNA–protein complexes were separated on a 6% DNA retardation gel (Invitrogen) in 0.5× TBE at 250 V for 1 hr. The gel was dried and exposed to a phosphoimager screen for 4 hr and then scanned by a phosphoimager.

2.3. Immunoprecipitation, Western and Southwestern blots

The immunoprecipitation assay has been described in our published paper [22]. Each immunoprecipitate (12 μL) was separated and transferred to a PVDF membrane. Immunoblotting was performed by incubation with the corresponding antibody and a Western blot procedure followed.

For the Western blot, blocking buffer (1% I-block™ reagent and 0.1% Tween-20) was employed as a blocking and washing buffer. Following sequential blockage with primary (1:200 diluted) and secondary (1:2000 diluted) antibodies, a thin layer of CSPD® ready-to-use substrate solution (Applied Biosystem) was transferred over the membrane. After incubation for 5 min, the membrane was exposed to an X-ray film for 3 min.

For the Southwestern blot, both the transfer and binding reactions were performed at 4°. PVDF membranes were incubated overnight with 1×10^6 cpm/mL [γ ^{32}P]ATP end-labeled consensus oligonucleotides in 1% I-block™ blocking buffer. After washing twice with 0.5% I-block™ blocking buffer, membranes were exposed to a phosphoimager screen for 18 hr and scanned by a phosphoimager.

2.4. Confocal microscopy

We have described the protocol of confocal microscopy analysis in our previous study [22]. Specimens were incubated with 2 μg/mL primary antibodies (Santa Cruz) of NF-Y subunits A (rabbit), B (goat) or C (goat) for 60 min. After three washes, cover slips were incubated with FITC-conjugated goat anti-rabbit (5 μg/mL) and Rhodamine conjugated bovine anti-goat (5 μg/mL) secondary antibodies (Santa Cruz) in a dark chamber for 45 min, followed by three washes with PBS. Cover slips were mounted and examined with a confocal microscope using the appropriate filters.

2.5. Measurement of [^{3}H]-labeled Gemcitabine incorporate into DNA

About 5×10^5 cells were plated on 35-mm dishes and then treated with 0.1 mM of hydroxyurea or 100 ng/mL of TSA. At the indicated time point, 7 μL of [^{3}H]-labeled Gem (3.5 μCi/mL, 0.25 nmol/mL) was added, and the cells were incubated for 30 min at 37° in a humidified atmosphere containing 5% carbon dioxide. The QIAamp® DNA mini Kit (Qiagen) was employed to extract DNA for each sample. The radioactivity of each 10 μg of DNA was measured using a Beckman LS 5000 CE liquid scintillation counter.

2.6. Ribonucleotide reductase activity and dCTP pool assay

The RR activity assay has been described in detail [23]. Briefly, the reaction mixture contained 0.15 μM of [^{3}H]CDP, 50 mM of HEPES (pH 7.2), 6 mM of DTT, 4 mM of magnesium acetate, 2 mM of ATP, and 0.05 mM of CDP, and a specific amount of cell lysate. The mixtures were incubated at 37° for 20 min. The formed dCDP and remaining CDP were dephosphorylated by phosphodiesterase. Then, cytidine and deoxycytidine were separated with a C18 ion exchange column by HPLC.

The dCTP pool assay has been optimized and described in our previous study [23]. About 1×10^6 cells pellets were harvested and added with 100 μL of 15% trichloroacetic acid. The supernatants were saved and extracted with two 50 μL aliquots of 1,1,2-trichlorotri-fluoroethane/trioctylamine (55%:45%). The reaction mixture (50 μL) of assay contained 50 mM of Tris–HCl (pH 7.5), 10 mM of $MgCl_2$, 5 mM DTT, 0.25 μM of [^{3}H]dATP, 0.2 units of sequenase, and a diluted sample. After incubation for 20 min, 40 μL of aliquots were spotted onto circular Whatman DE81 ion exchange papers. Samples were counted in a liquid scintillation counter and compared to a standard sample prepared in the presence of 0, 0.25, 0.5, 0.75 and 1.0 pmol/μL of each dCTP.

2.7. HDAC activity assay

The HDAC assay kit is commercially available from Upstate Biotechnology. Briefly, the biotinylated histone H4 peptide was acetylated with [^{3}H]acetylCoA, and captured by streptavidin agarose. [^{3}H]Acetate-labeled histone H4 peptide was incubated with 20 μg of nuclear extracts in

HDAC assay buffer for 24 hr. The released [^{3}H]acetate was separated by centrifugation. Relative HDAC activity was equal to the percentage of [^{3}H]acetate released from H4 peptide.

2.8. Microarray analyses

The mRNA isolation, cRNA preparation, microarray hybridization and data analysis has been described in our previous publication [24]. The HG-U95Av2 microarray set from Affymetrix was employed to analyze the gene mRNA expression. The analyses were performed at the Microarray Core Facility, Children's Hospital Los Angeles. The data was analyzed using Affymetrix Microarray Software Suite (v.4.0) and GeneSpring™ (v5.0) software (Silicon Genetics). The quality of hybridization was evaluated with internal control spots. Each chip was normalized with the standard protocol of the core facility. Spots representing housekeeping genes were further used to normalize the entire slide so that all slides could be compared directly.

3. Results

3.1. Upregulation of hRRM2 promoter activity and overexpression of hRRM2 in KBGem

From Fig. 1A and B, there was not only an increased expression of *hRRM2* subunits, but also a significant increase of the *hRRM2* protein that co-immunoprecipitated with agarose-conjugated *hRRM1* antibody of the KBGem clone. The amount of *p53R2* protein pulled down by the *hRRM1* antibody changed slightly in the KBGem clone. As with the increase of *hRRM2*, the RR activity of KBGem was significantly higher than that of KB (Fig. 1C), and IC_{50} of Gem escalated almost 100-fold in KBGem clone. This indicated that overexpression of the *hRRM2* subunit rather

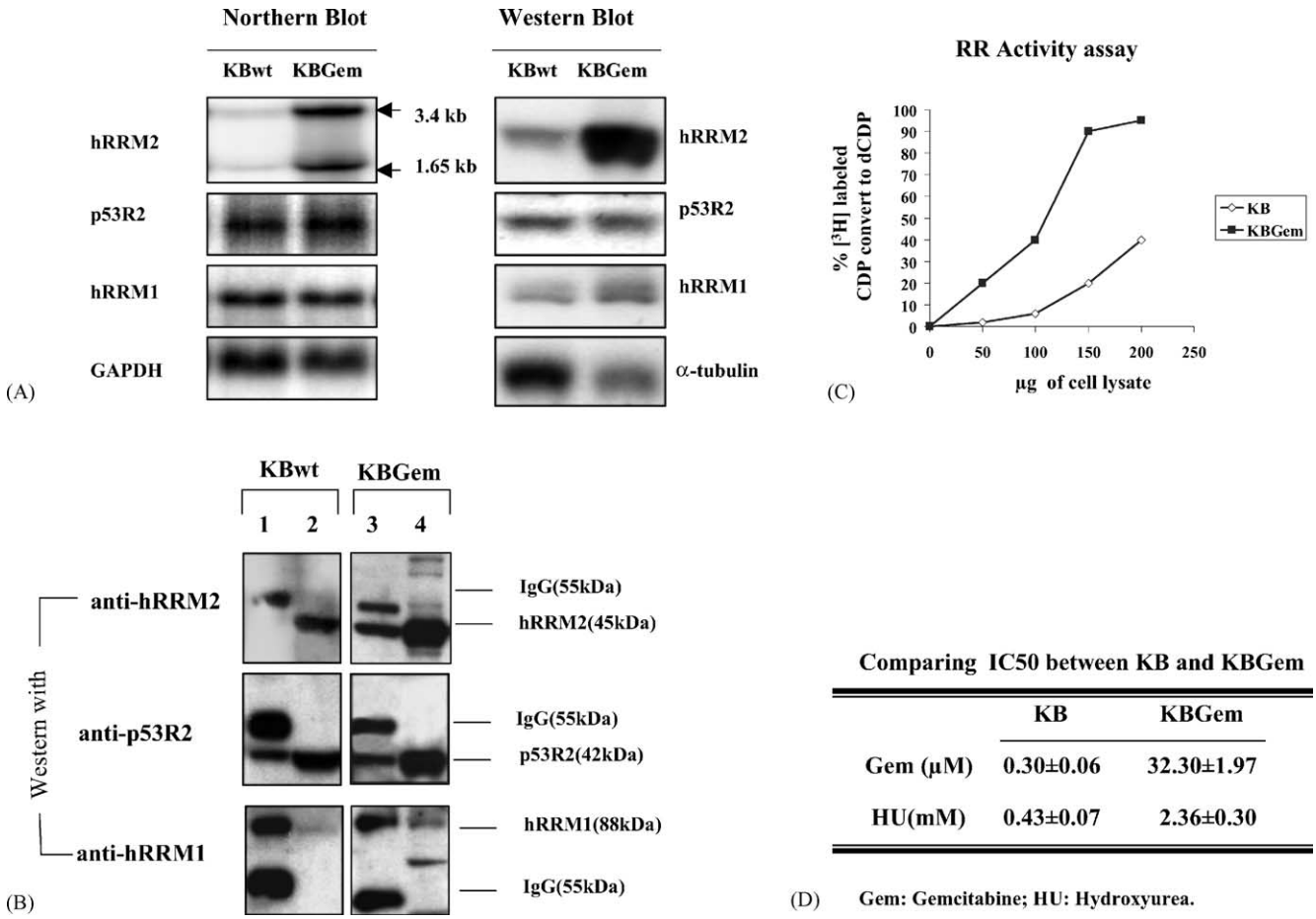

Comparing IC50 between KB and KBGem

	KB	KBGem
Gem (μM)	0.30±0.06	32.30±1.97
HU(mM)	0.43±0.07	2.36±0.30

(D) Gem: Gemcitabine; HU: Hydroxyurea.

Fig. 1. hRR subunits expression and RR activity in KB cells and KBGem clones. (A) Northern blot: 20 μg of total RNA were separated in each lane. Blots were hybridized with a [^{32}P]-labeled *hRRM2*, *hRRM1* and *p53R2* full-length cDNA probe [16]. Western blot: total cell lysates from KB and KBGem clone were separated by 10% SDS–PAGE. (B) Immunoprecipitation Western blot: immunoprecipitates of KB and KBGem were loaded to lanes 1 and 3; and 70 μg of KB and KBGem lysates were added to lanes 3 and 4 as control, respectively. Immunoblotting was performed by incubation with the corresponding antibody and followed by Western blot. (C) RR activity: the percentage of [^{3}H]-labeled CDP reduced to dCDP was used instead of relative RR activity. The amount of 50, 100, 150 and 200 μg, of cell lysate from KB and KBGem were applied to detect RR activity, respectively. (D) IC_{50} was based on the colony formation assay [15].

than *hRRM1* or *p53R2* might contribute to form additional $\alpha_2\beta_2$ heterotetramers, which are required for RR activity in the KBGem clone.

A 10.3 kbp *hRRM2* genomic DNA fragment containing 2.8 kbp of the promoter region has been sequenced and published (GenBank accession number AY032750) [17]. The sequence was analyzed and binding sites for putative transcription factors were identified in Fig. 2A. There are two transcription start points (Tsp) in the *hRRM2* promoter, leading to two separable promoter regions: a proximal promoter region (Pa) and a distal promoter region (Pb). Several putative transcriptional binding sites were found in Pb, including sites for NF-κB, E2F, AP-1 and OCT-1, etc. Thus, the Pa region includes a TTTAAA sequence (TATA-like box) and three CCAAT sequences.

As shown in Fig. 2B, relative luciferase activity for reporter constructs showed significant increases as the promoter extended from P1 to P3 in both KB and KBGem clones; but from P3 to P5, no increased luciferase activity could be identified. The reporter constructs of P1 and pGL3-basic failed to show a significant difference between KB and KBGem. The reporter construct of P2, containing one CCAAT box and a TATA box, was upregulated 2-fold of the promoter activity in KBGem; the relative luciferase activity of P3, P4 and P5, which contain three CCAAT boxes, increased almost 4–5-fold in KBGem.

As shown in Fig. 2C, right panel, the relative luciferase activities of Pα with three sequential CCAAT boxes were up-regulated almost 5-fold in KBGem, and were steadily reduced as the mutation number of CCAAT boxes increased compared to activities in KB cells. While all three CCAAT boxes were mutated, the relative luciferase activity showed no significant difference between KBGem and KB. With regards to reporter constructs of PB1, PB2, PB3 and PB4, no increased relative luciferase activity in KBGem was found. However, the relative luciferase activity of construct PB2 in KBGem was only half as active as in KB.

3.2. Interaction between NF-Y and CCAAT elements of hRRM2 proximal promoter region

As shown in Fig. 3, two major DNA–protein complexes were detected in a gel shift assay (bands c and d) when nuclear extract from KB (Fig. 3A) or KBGem (Fig. 3B) cells was incubated with γ ^{32}P labeled Pα12 (lane 2). These bands were prevented from forming in an excess of unlabeled Pα12 (lanes 3–5), but not PαMut12 (lanes 6–8). Both complexes of bands (a) and (b) were super-shifted by anti-NF-YA and NF-YB antibodies (lanes 9 and 10). In addition, the same results were shown when we used γ ^{32}P labeled Pα23 instead of Pα12 (data is not shown). Taken together, these results indicate that NF-Y specifically interacts with the *hRRM2* Pα region CCAAT boxes to form DNA–protein complexes. Furthermore, nuclear extracts from KB and KBGem interacted differently with Pα12 by forming different binding patterns. Incubation in KB extract produced more of the complex labeled band c, while the KBGem extract generated more of the complex labeled band d. Band c was barely detectable when the KBGem extract was incubated with Pα12. These results suggest that NF-Y subunits might form different configurations between KB and KBGem cells.

3.3. The heterotrimer assembly of NF-Y and its translocation

A Western and Southwestern blot was used to confirm the specific binding of the *hRRM2* proximal promoter region to NF-Y in KB and KBGem extracts as shown in Fig. 4. Only one major band, designated as 114 kDa, was identified in both cell extracts when probed by either labeled DNA fragment (Fig. 4, lanes 1–6). As reported in a previous study, *NF-YA*, *NF-YB* and *NF-YC* were supposed to assemble as a functional 114 kDa NF-Y heterotrimer complex [25]. From Fig. 4 (lanes 7–12), only the bands of 114 kDa could be stained with antibodies against *NF-YA*, *NF-YB* and *NF-YC*. Besides 114 kDa, the band of 43 kDa (P43)—regarded as an isolated NF-Y subunit A—could be detected with the anti-NF-YA antibody. However, *p43* could not be probed with a radiation labeled consensus sequence. These results suggested that NF-Y bound to the CCAAT box as a heterotrimer but not as an individual subunit. Although the amount of NF-Y that was detected in extracts from KBGem did not show a significant increase compared to KB, a greater amount of labeled DNA probe bound to NF-Y from KBGem than from KB (lanes 2, 4, 6 vs. lanes 1, 3, 5). *NF-YA* only interacts with the NF-YB:C heterodimer, but not with *NF-YB* or *NF-YC* alone, to form the NF-Y heterotrimer, which then interacts with CCAAT boxes to regulate downstream gene expression [19].

To further examine the distribution of NF-Y subunits, confocal microscopy was employed to show co-localization of *NF-YA* with the NF-YB:C heterodimer in KB and KBGem cells as shown in Fig. 5. In KB cells, NF-Y subunits A, B and C were localized in both the cytoplasm and the nucleus, with most of the subunits distributed between the cytoplasm and the nucleus. *NF-YA* co-localized with NF-YB:C at the edge of the nucleus to form an eccentric aggregation pattern in KB cells (see arrows in Fig. 5). In KBGem cells most of the *NF-YA* co-localized with NF-YB:C at the interior of the nucleus, which confirmed that the functional NF-Y heterotrimer was higher than in KB cells. The above results implied that the assembly of NF-Y subunits might modulate NF-Y affinity to CCAAT boxes.

3.4. Trichostatin A, NF-Y transactivation and hRRM2 expression

The HDAC had been reported to depress the NF-Y transactivation [21]. TSA, a HDAC inhibitor, was

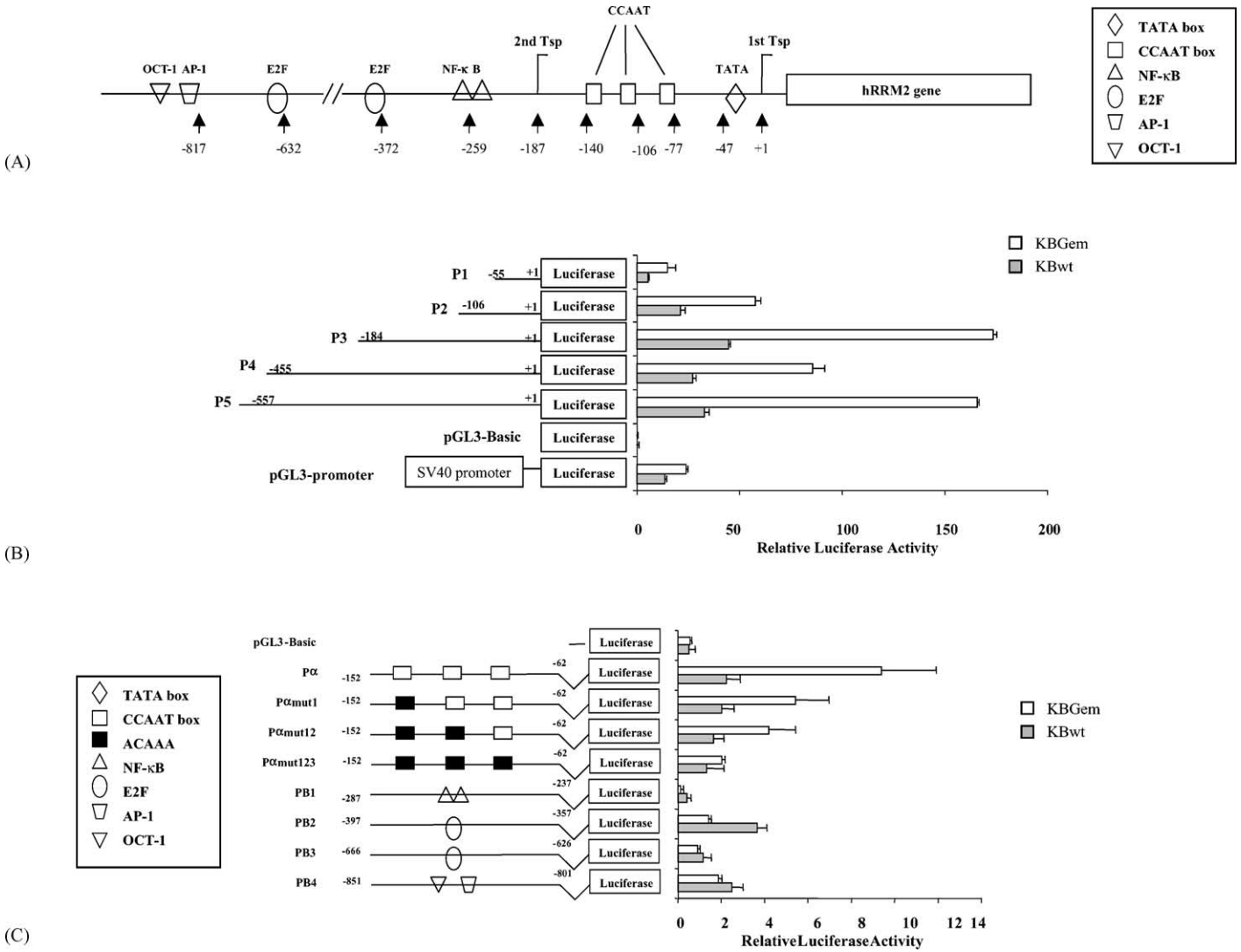

Fig. 2. Transcription activity of the *hRRM2* promoter region in KB and KBGem clones. The relative luciferase activity was adjusted by β-galactosidase and protein concentration. All samples were detected with three duplicates; and Student's *t*-test was applied to analyze the statistical significance. (A) Putative transcriptional binding sites were predicted in the *hRRM2* promoter region. (B) and (C) The left panel indicated the luciferase reporting vectors containing the corresponding fragments. The right panels showed the value of relative luciferase ($^{*}P < 0.05$, compare KBGem with KB).

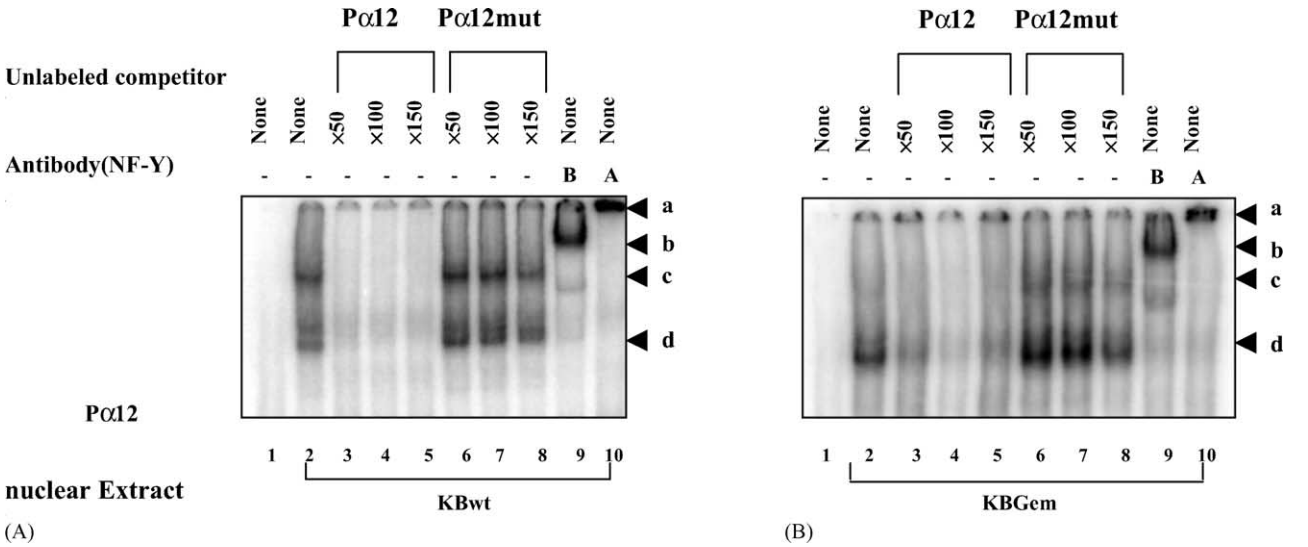

Fig. 3. Electrophoretic mobility shift assays. Lane 1 is a negative control; only loaded 0.035 pmol [^{32}P] end-labeled Pα12. Lanes 2–10: contained labeled Pα12, and 4 μg nuclear extracts from KB and KBGem in left and right panel, respectively. Excess unlabeled oligonucleotide (Pα12 or PαMut12) was added as a competitor to show specificity. 50-fold excess was added to lanes 3 and 6, 100-fold to lanes 4 and 7, and 150-fold to lanes 5 and 8. In lanes 9 and 10, antibodies to *NF-YB* and *NF-YA* were added to supershift complexes and confirm the presence of NF-Y in the binding complex.

employed to investigate whether the upregulation of NF-Y might change the RR subunits' expression in KB cells. From Fig. 6A, HDAC activity of KBGem (22.08%) was significantly lower than KB cells (62.55%) ($P < 0.01$). After treatment with 100 ng/mL TSA, the HDAC activity was inhibited at the time points 2, 4, 6 and 8 hr in KB cells. As with the inhibition of HDAC, the luciferase activity of Pα, rather than CCAAT boxes, mutated PαMut and caused a significant increase after treatment with TSA for 24 hr (Fig. 6B). Moreover, the expression of *hRRM2* eventually increased at the time point of 4, 6, 8, and 24 hr (Fig. 6C). Nevertheless, the *hRRM1* and *p53R2* failed to show a significant change after treatment with TSA (Fig. 6C).

The dCTP pool assay and [^{3}H]-labeled Gem incorporation assay were employed to investigate whether increased *hRRM2* would affect Gem incorporation into DNA. Hydroxyurea (0.1 mM) was employed as a positive control, since it is known to enhance Gem incorporation into the DNA, which is mediated by inhibiting *hRRM2* subunit protein [26]. From the results shown in Fig. 6D, after treatment with 100 ng/mL TSA, the dCTP pool almost doubled at the time point of 2, 4, 6 and 8 hr. It decreased steadily when exposed to hydroxyurea. Meanwhile, the incorporated

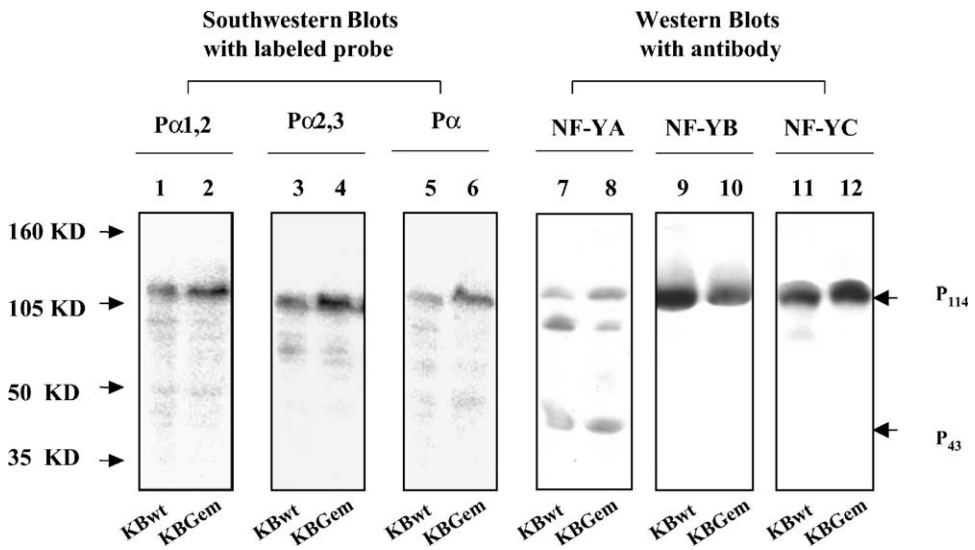

Fig. 4. Southwestern and Western blot analysis. Extracts in odd lanes (1, 3, 5, 7, 9 and 11) are from KB cells, and even lanes (2, 4, 6, 8, 10 and 12) are from KBGem. Separation and transferring of nuclear extracts (150 μg) were performed at 4°, avoiding heat. Lanes 1–6 were probed with end labeled fragments of Pα12 (lanes 1 and 2), Pα23 (lanes 3 and 4), or Pα (lanes 5 and 6). Lanes 7–12 show Western blots probed with antibodies of anti-*NF-YA* (lanes 1 and 8), *NF-YB* (lanes 9 and 10) and *NF-YC* (lanes 11 and 12).

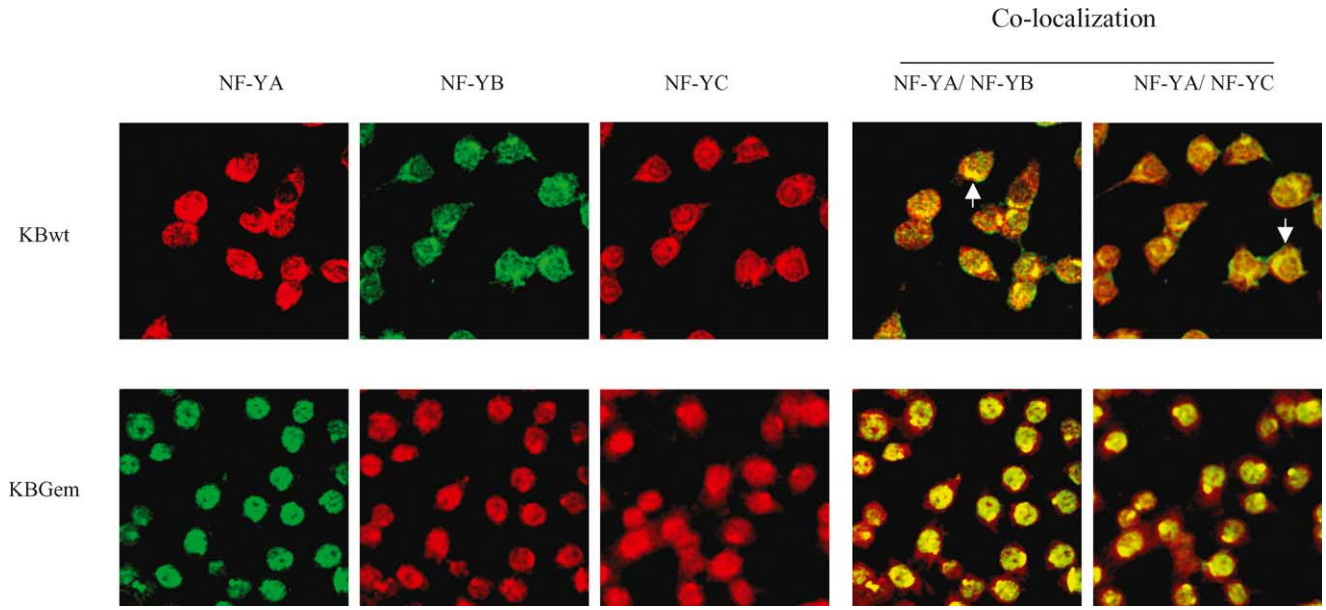

Fig. 5. Co-localization of NF-Y subunits A, B, and C. Confocal microscopy was performed as described in Section 2. Overlays of *NF-YA* with *NF-YB* or *NF-YC* are shown on the top and bottom panel for KB and KBGem, respectively.

[^{3}H]-labeled Gem, increased steadily after exposure to hydroxyurea, but it decreased steadily in a time-dependent manner under treatment with TSA.

3.5. Microarray analysis of genes' expression of KB and KBGem clone

Microarray was employed to further analyze genes expression change in the KBGem clone. After the Gem selection procedure, numerous genes changed in the drug resistant clone, but most of these changed genes had no apparent relationship to the Gem resistance mechanism (data not shown). Therefore, we focused on investigating those genes that might be related to Gem metabolism or NF-Y regulation.

Besides the *hRRM2*, the cytidine metabolism-related genes were reported to play a critical role in Gem resistance [7,8,11,13–15]. From the results of the microarray analysis (Table 1, second panel), *hENT1* decreased 4.31-fold, and *CDA* increased 1.48-fold in KBGem when compared to KB parental cells, while expression of *5′-Nucl* had almost no change. Our previous finding has demonstrated that there was no significant difference in the *DCK* expression between KB and the KBGem clone [15].

Most of the HATs were upregulated in the KBGem clone, and the *P300/CBP* was upregulated almost 10-fold. In contrast to HATs, most of the members of the HDAC, except HD1, were downregulated in KBGem, which was consistent with our findings on HDAC activity assay (Fig. 6A). It was suggested that the increased histone acetylation might contribute to the NF-Y transactivation in this KBGem clone.

Many human cell cycles or cell proliferation-related genes had been reported as regulating through CCAAT motifs located on their promoter region [19,27]. Microarray analysis results indicated that most of the above genes were upregulated in KBGem. In particular, the mRNA levels of *cdc25A*, *cyclin A*, *cyclin B*, DNA topoisomerase II, *E2F-1*, thymidine kinase and TGFβ receptor I, which were reported as containing CCAAT motifs in the promoter region, were upregulated to 2.73-, 2.19-, 1.49-, 2.01-, 1.88-, 2.72-, 3.33- and 4.64-fold, respectively. Only *cdc2*, which contained CCAAT motifs in the promoter, was downregulated 7.83-fold. The above results provided further evidence to support how NF-Y transactivation might be upregulated in this KBGem clone.

4. Discussion

Gemcitabine, an analogue of deoxycytidine, is widely used as a chemotherapeutic agent against human malignant disease. Many factors relating to Gem metabolism and transportation have been reported causing drug resistance [7], and increased RR activity has been regarded as one of the potential factors causing resistance to Gem [7,15,28]. The *hRRM2* overexpression has been reported to contribute to increased hRR activity in selected drug resistant clones of a nucleoside analogue (Gem) [15] and hRR inhibitors (hydroxyurea) [29,30]. Our previous study had demonstrated that the hRR subunit M2, but not M1, was sufficient to contribute to increased hRR activity and increased resistance to hydroxyurea in transfected KB cells [31]. Our group has demonstrated that a low dose of hydroxyurea, the *hRRM2* inhibitor, may temporarily arrest cells in the G1/0 phase. Once the cells escape, Gem incorporation increased. This phenomenon is unique and depends on the time and sequence [26]. The above indicates that the

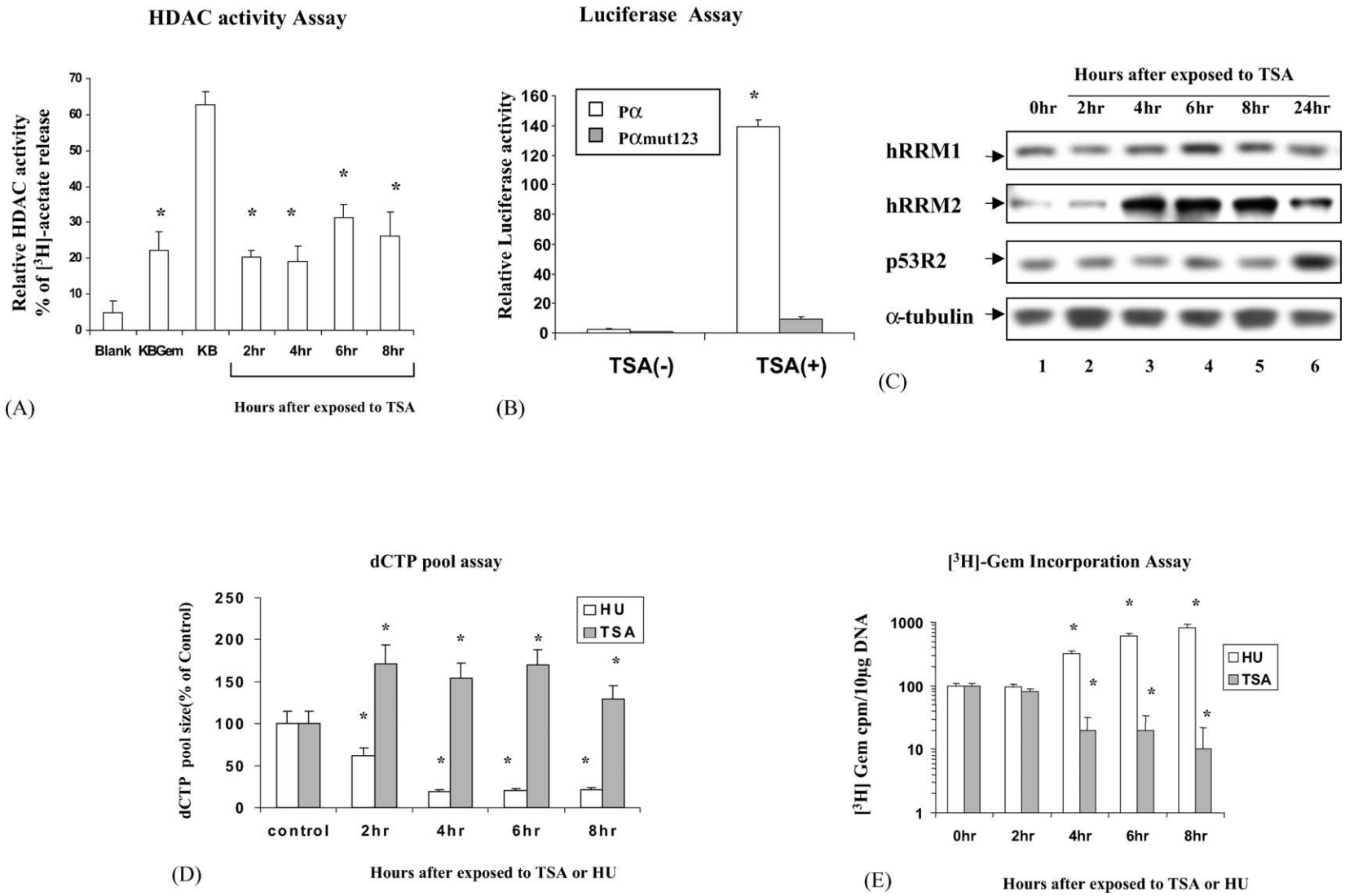

Fig. 6. HDAC inhibitor and *hRRM2* expression. (A) HDAC activity assay: the nucleus extracts of KBGem and KB cells, and KB cells after 2, 4, 6 and 8 hr exposed to 100 ng/mL of TSA were determined with an assay kit. Each sample had three duplicates. ($^*t$-test, $P < 0.01$, compare with KB). (B) Luciferase assay: 10 μg luciferase reporter constructs Pα (white block) and PαMut123 (gray block) were transfected into KB. The TSA(+)/TSA(−) were incubated with/without 100 ng/mL of TSA for 24 hr ($^*t$-test $P < 0.01$). (C) Western blot analysis: KB cells were harvested after incubation with 100 ng/mL of TSA for 2, 4, 6, 8, and 24 hr. The 40 μg of total lysate of KB was loaded to lane 1 as baseline control, and the above lysate extracted from TSA treated KB were added to lanes 2–6, respectively. (D) dCTP pool assay: under treatment with 100 ng/mL TSA (gray blocks) or 0.1 mM hydroxyurea (white blocks), the dCTP pools were determined as described in Section 2. (E) [^{3}H]-labeled Gem incorporation assay: [^{3}H]-labeled Gem was added to incubate the cells for 30 min at 0, 2, 4, 6 and 8 hr time points after exposure to 100 ng/mL TSA (gray blocks) or 0.1 mM hydroxyurea (white blocks). In panels D and E, each sample was repeated three times. The *t*-test was applied to analyze the statistical significance ($^*P < 0.05$, compare with control in D, with 0 hr time point in E).

Table 1
Microarray analysis of mRNA expression changing in KBGem clone

Affy prob-set	Genbank accession no.	Symbol	Ave Diff[a]		Fold change[b]
			KB	KBGem	
Genes for internal control					
32272_at	K00558	α-Tubulin	103940.6	103557.1	1.00
39331_at	X79535	β-Tubulin	1411.4	1413.8	1.00
32318_s_at	X63432	Mutant β-actin	11657.0	9652.5	−1.21
41753_at	U48734	Non-muscle α-actinin	33548.1	38331.5	1.14
Genes related to Gem metabolism					
33901_at	U81375	hENT1	4011.8	930.0	−4.31
1117_at	L27943	Cytidine deaminase	2863.5	4237.1	1.48
31794_at	D38524	5-Nucleotidase	1412.4	1487.4	1.05
886_at	M60527	Deoxycytidine kinase	Absent	62.7	–
Histone acetyltransferase (HAT)					
41855_at	AF030424	Histone acetyltransferase 1	1476.0	1381.8	−1.07
34231_at	AF074606	Histone acetyltransferase (HBO1)	5441.7	6843.8	1.26
38628_at	AF029777	Histone acetyltransferase (GCN5)	1045.9	1813.2	1.73
1012_at	U57317	P300/CBP	54.2	567.7	10.47
33810_at	AF110377	PCAF400	82.0	218.4	2.66
Histone deacetylase (HDACs) and HDAC1 complex subunits					
476_s_at	U50079	Histone deacetylase HD1	60.0	293.6	4.89
39358_at	U37146	SMRT	1364.7	721.4	−1.89
33859_at	U96915	SAP18	5569.2	2092.5	−2.66
38771_at	D50405	Histone deacetylase 1	2264.7	248.6	−8.80
34368_at	U31814	Histone deacetylase 2	312.0	202.7	−1.49
35821_at	U75697	Histone deacetylase 3	55.7	57.8	1.07
38271_at	AB006626	Histone deacetylase 4	183.2	72.4	−2.44
38810_at	AF039241	Histone deacetylase 5	570.6	226.7	−2.43
35795_at	AJ011972	Histone deacetylase 6 (JM21)	2389.6	1192.1	−2.00
Proliferation related genes					
1803_at	X05360	cdc2[c]	1626.6	207.8	−7.83
1738_at	M81933	cdc25A	925.8	2527.2	2.73
1584_at	M34065	cdc25Hs	473.8	1038.3	2.19
1942_s_at	U37022	cdk4	930.6	1149.1	1.23
1943_at	X51688	Cyclin A[c]	492.7	734.1	1.49
1945_at	M25753	Cyclin B[c]	1513.3	3037.5	2.01
2017_s_at	M64349	Cyclin D1	492.2	2232.7	4.54
1983_at	X68452	Cyclin D2	3581.2	4408.4	1.23
1795_g_at	M92287	Cyclin D3	33113.3	33511.1	1.01
2021_s_at	M73812	Cyclin E	257.9	791.2	3.07
1925_at	Z36714	Cyclin F	2792.2	4261.2	1.53
1913_at	U47414	Cyclin G2	395.4	64.8	−6.10
1924_at	U11791	Cyclin H	2528.5	2971.0	1.18
1836_at	D50310	Cyclin I	37625.9	10979.5	−3.43
36391_at	AF048730	Cyclin T1	1311.3	807.7	−1.62
32053_at	AF048731	Cyclin T2a	127.5	120.9	−1.05
1592_at	J04088	DNA topoisomerase II[c]	1062.4	1997.4	1.88
36571_at	X68060	DNA topoisomerase IIb	5633.9	1515.0	−3.72
1028_at	U43431	DNA topoisomerase III	1368.5	1691.6	1.24
1775_at	L24559	DNA polymerase α	3302.7	5658.5	1.71
1696_at	D29013	DNA polymerase β	2238.6	5668.7	2.53
41085_at	AF025840	DNA polymerase ε b	551.3	869.9	1.58
1726_at	N/A	DNA polymerase, ε, catalytic subunit	372.0	1209.3	3.25
1322_at	U47677	E2F-1*	933.4	2542.7	2.72
38707_r_at	S75174	E2F-4	10745.2	11860.3	1.10
1703_g_at	S75174	E2F-4	1363.7	2054.4	1.51
1044_s_at	U31556	E2F-5	156.8	92.1	−1.70
41400_at	K02581	Thymidine kinase[c]	1232.4	4103.4	3.33
383_at	X70340	TGFα	316.0	662.3	2.10
41445_at	X02812	TGFβ	10172.4	13501.0	1.33
1767_s_at	X14885	TGFβ3	1111.9	1283.3	1.15
38374_at	AF050110	TGFβ inducible early protein and early growth response protein α	14.6	23.1	1.58
32714_s_at	L17075	TGFβ receptor[c]	250.8	1162.5	4.64
1495_at	M34057	TGFβ 1 binding protein	155.9	230.9	1.48

[a] Ave Diff: average difference; the average difference values representing perfect match subtracting mismatch for each gene were normalized after scaling the standard chip intensities to an average of 1500 units.

[b] Fold change: if Ave Diff (KB) < Ave Diff (KBGem), fold change: Ave Diff (KBGem)/Ave Diff (KB); if Ave Diff (KB) > Ave Diff (KBGem), fold change = (−1) (Ave Diff (KB)/Ave Diff (KBGem)).

[c] Genes have been reported containing CCAAT motif in the promoter region [19,27,32,38,39].

overexpression of RR small subunit M2 might predominantly contribute to increased RR activity and plays a key role in this Gem drug resistant clone. It also implied that applications of small interfering RNA (siRNA) or antisense RNA that target *hRRM2* might enhance Gem sensitivity.

Gene amplification of *hRRM2* was one of the key points causing overexpression of *hRRM2* in KBGem [16], but it could not fully explain the almost 30-fold mRNA increase and Gem resistant mechanism in the KBGem clone. Results from this study revealed the transcription activity of the three CCAAT boxes of the *hRRM2* proximal promoter had been up-regulated almost 5-fold in KBGem (Fig. 2B and C). However, no mutation has been detected in the *hRRM2* proximal promoter region in the KBGem clone. This finding first elucidates that increased transactivation of the *hRRM2* proximal promoter, which contained three CCAAT boxes, might be related to Gem resistance in a selected clone.

The CCAAT box is a common element of RNA polymerase II promoters in eukaryotic cells and is often found between 80 and 100 base pairs upstream of the transcription start site. About 30% of eukaryotic promoters of tissue-specific, house keeping and cell cycle regulation classes of genes have the CCAAT motif, G/AG/ACCAAT/GA/GC/G [16,19]. In several promoters, the sequence around the CCAAT box and the spacing between the CCAAT box and other specific elements is conserved between species [19,32]. CBF/NF-Y has been shown to bind to more than 150 CCAAT-containing promoters, and requires the 5-nucleotide sequence CCAAT [32]. NF-Y subunits from KB and KBGem clones could interact with the *hRRM2* proximal promoter, CCAAT motifs, to form different binding patterns between them (Figs. 3–5). It was suggested that NF-Y binding to the CCAAT motif and transactivation of the *hRRM2* proximal promoter might be modulated by an alteration of the NF-Y subunits assembly in the KBGem clone. The human histone acetyltransferases *GCN5* and *P/CAF* might serve to modulate NF-Y transactivation by disrupting local chromatin structure and facilitating NF-Y access to DNA binding sites [33]. The finding from the microarray analysis revealed that most of the HAT family members were upregulated and that HDAC complex members were downregulated in the KBGem clone. The HDAC activity inhibition in KBGem was further confirmed by HDAC activity assay (Fig. 6A). Furthermore, under treatment with TSA, a HDAC inhibitor, NF-Y transactivation was induced, which resulted in an increase of *hRRM2* expression and expansion of dCTP. Expansion of the dCTP pool caused abrogation of [^{3}H]Gemcitabine incorporation in KB cells. However, we need to further investigate whether TSA would reduce Gem sensitivity, since TSA might cause cytotoxicity through another pathway besides inhibition of HDAC. Nevertheless, our finding confirmed that NF-Y was positively and negatively regulated by HAT and HDAC, respectively.

It is well known that the promoters of many human cell cycles and cell proliferation-related genes contain CCAAT motifs (such as topoisomerase II, thymidine kinase, *cdc25C*, *cyclin A*, *cyclin B*, *cyclin B2* and *cdk1c*) [19,27,32]. Therefore, upregulation of NF-Y transactivation may change the biological behavior that includes cell proliferation, DNA repair, and invasive and metastases potential in drug resistance clones. From a microarray analysis, most proliferation-related genes were upregulated, which further confirmed the increase of NF-Y transactivation in KBGem. Increasing the RR subunit R2 may increase the genomic instability in a mouse cell line [34]. Furthermore, our previous results have shown that overexpression of *hRRM2* drug resistant clones have greater invasive potential [35]. Thus, it is implied that NF-Y inhibitors may not only reverse resistance to Gem but may also prevent aggressive potential in the KBGem clone.

Along with overexpression of hRR, deficiency of the *hENT1* [7,8], increased activity of nucleases [11], and loss of expression of *DCK* [13,14] have been reported as essential factors of Gem resistant mechanisms. Our findings from microarray analyses indicated that decreased *hENT1* and increased *CDA* might also play a role in this selected Gem resistant KB clone. Reduced expression of *hENT1* might limit Gem transportation and improved expression of *CDA* might accelerate Gem degradation, which would enhance drug resistance. Many factors might involve in expression regulation of *hENT1* and *CDA* during the drug selection procedure. Nevertheless, the expanding dNTP pool caused by overexpression of RR activity might inhibit the expression of *hENT1* and enhance the *CDA* activity to limit dNTP pool in a feedback manner in KBGem.

It was reported that increase of RR is related to the regulation of the 3′-untranslated region (3′UTR) of mRNA in hydroxyurea drug resistant clones [36]. [Studies have found the growth factor, cytokines, tumor promoters and oxidation/reduction agents might modulate the mouse ribonucleotide reductase large and small subunits' mRNA binding protein via modulating the transformation growth factor β (TGFβ) or protein kinase C (*PKC*) pathway, which affect the mRNA stability [36,37].] Interestingly, the transformation growth factor β receptor II gene (*TGFβR II*) was reported to have transcriptional regulation by NF-Y [38]. Microarray results showed both TGFβ and TGFβ receptor II were upregulated in KBGem. TGFβ would regulate P75 binding 3′UTR of mouse R2 mRNA to avoid digestion by nuclease through activation of the effector Smad [36]. It was suggested that increasing NF-Y might not only upregulate RRM2 transcripts directly, but also enhance the *hRRM2* mRNA stability by regulating the TGFβ pathway in KBGem.

In summary, this study extended the hypothesis that *hRRM2* overexpression, which caused Gem resistance in KBGem clones, was regulated by improved NF-Y transactivation. It was implied that inhibitors of NF-Y might

reduce the *hRRM2* expression and further enhance the nucleoside analogues drug sensitivity.

Acknowledgments

This study was financed by National Institute of Health (NIH) RO-1 grant (CA 72767).

References

[1] Jordan A, Reichard P. Ribonucleotide reductases. Annu Rev Biochem 1998;67:71–98.
[2] Rova U, Adrait A, Pötsch S, Gräslund A, Thelander L. Evidence by mutagenesis that Tyr (370) of the mouse ribonucleotide reductase R2 protein is the connecting link in the intersubunit radical transfer pathway. J Biol Chem 1999;274:23746–51.
[3] Tanaka H, Arakawa H, Yamaguchi T, Shiraishi K, Fukuda S, Matsui K, Takei Y, Nakamura Y. A ribonucleotide reductase gene involved in a *p53*-dependent cell-cycle checkpoint for DNA damage. Nature 2000; 404:42–9.
[4] Nakano K, Balint E, Ashcroft M, Vousden KH. A ribonucleotide reductase gene is a transcriptional target of *p53* and *p73*. Oncogene 2000;19:4283–9.
[5] Yamaguchi T, Matsuda K, Sagiya Y, Iwadate M, Fujino MA, Nakamura Y, Arakawa H. *p53R2*-dependent pathway for DNA synthesis in a *p53*-regulated cell cycle checkpoint. Cancer Res 2001;61: 8256–62.
[6] Guittet O, Häkansson P, Voevodskaya N, Gräslund A, Arakawa H, Nakamura Y, Thelander L. Mammalian *p53R2* protein forms an active ribonucleotide reductase *in vitro* with the R1 protein, which is expressed both in resting cells in response to DNA damage and in proliferating cells. J Biol Chem 2001;276:40647–51.
[7] Galmarini CM, Mackey JR, Dumontet C. Nucleoside analogues: mechanisms of drug resistance and reversal strategies. Leukemia 2001;15:875–90.
[8] Mackey JR, Jennings LL, Clarke ML, Santos CL, Dabbagh L, Vsianska M, Koski SL, Coupland RW, Baldwin SA, Young JD, Cass CE. Immunohistochemical variation of human equilibrative nucleoside transporter 1 protein in primary breast cancers. Clin Cancer Res 2002;8:110–6.
[9] Plunkett W, Huang P, Xu YZ, Heinemann V, Grunewald R, Gandhi V. Gemcitabine: metabolism, mechanisms of action, and self-potentiation. Semin Oncol 1995;22:3–10.
[10] Heinemann V, Hertel LW, Grindey GB, Plunkett W. Comparison of the cellular pharmacokinetics and toxicity of 2′,2′-difluorodeoxycytidine and 1-β-D-arabinofuranosylcytosine. Cancer Res 1988;48:4024–31.
[11] Hunsucker SA, Spychala J, Mitchell BS. Human cytosolic 5'-nucleotidase I: characterization and role in nucleoside analog resistance. J Biol Chem 2001;276:10498–504.
[12] Heinemann V, Xu YZ, Chubb S, Sen A, Hertel LW, Grindey GB, Plunkett W. Inhibition of ribonucleotide reduction in CCRF-CEM cells by 2′,2′-difluorodeoxycytidine. Mol Pharmacol 1990;38:567–72.
[13] Gourdeau H, Clarke ML, Ouellet F, Mowles D, Selner M, Richard A, Lee N, Mackey JR, Young JD, Jolivet J, Lafrenière RG, Cass CE. Mechanisms of uptake and resistance to troxacitabine, a novel deoxycytidine nucleoside analogue, in human leukemic and solid tumor cell lines. Cancer Res 2001;61:7217–24.
[14] Ruiz van Haperen VW, Veerman G, Eriksson S, Boven E, Stegmann AP, Hermsen M, Vermorken JB, Pinedo HM, Peters GJ. Development and molecular characterization of a 2,2-difluorodeoxycytidine resistant variant of the human ovarian carcinoma cell line A2780. Cancer Res 1994;54:4138–43.
[15] Goan YG, Zhou BS, Hu E, Mi S, Yen Y. Overexpression of ribonucleotide reductase as a mechanism of resistance to 2,2-difluorodeoxycitidine in the human KB cancer cell line. Cancer Res 1999;59: 4204–7.
[16] Zhou BS, Mo XL, Liu XY, Qiu WH, Yen Y. Human ribonucleotide Reductase M2 subunit gene amplification and transcriptional regulation in a homogeneous staining chromosome region responsible for the mechanism of drug resistance. Cytogenet Cell Genet 2001;95:34–42.
[17] Zhou BS, Yen Y. Characterization of the human ribonucleotide reductase M2 subunit gene Genomic structure and promoter analyses. Cytogenet Cell Genet 2001;95:52–9.
[18] Park JB, Levine M. Characterization of promoter of the human ribonucleotide reductase R2 gene. Biochem Biophys Res Commun 2000;267:651–7.
[19] Maity SN, de Crombrugghe B. Role of the CCAAT-binding protein CBF/NF-Y in transcription. Trends Biochem Sci 1998;23:174–8.
[20] Kim IS, Sinha S, de Crombrugghe B, Maity SN. Determination of functional domains in the C subunit of the CCAAT-binding factor (CBF) necessary for formation of a CBF-DNA complex: CBF-B interacts simultaneously with both the CBF-A and CBF-C subunits to form a heterotrimeric CBF molecule. Mol Cell Biol 1996; 16:4003–13.
[21] Jin S, Scotto KW. Transcriptional regulation of MDR1 gene by histone acetyltransferase and deacetylase is mediated by NF-Y. Mol Cell Biol 1998;18:4377–84.
[22] Xue L, Zhou B, Liu X, Qiu W, Jin Z, Yen Y. Wild-type *p53* regulates human ribonucleotide reductase by protein–protein interaction with *p53R2* as well as *hRRM2* subunits. Cancer Res 2003;63:980–6.
[23] Zhou BS, Ker R, Ho R, Yu J, Zhao YR, Shih J, Yen Y. Determination of deoxyribonucleoside triphosphate pool sizes in ribonucleotide reductase cDNA transfected human KB cells. Biochem Pharmacol 1998;55:1657–65.
[24] Qiu W, David D, Zhou B, Chu PG, Zhang B, Wu M, Xiao J, Han T, Zhu Z, Wang T, Liu X, Lopez R, Frankel P, Jong A, Yen Y. Down-regulation of growth arrest DNA damage-inducible gene 45β expression is associated with human hepatocellular carcinoma. Am J Pathol 2003;162:1961–74.
[25] Lum LS, Sultzman LA, Kaufman RJ, Linzer DI, Wu BJ. A cloned human CCAAT-box-binding factor stimulates transcription from the human hsp70 promoter. Mol Cell Biol 1990;10:6709–17.
[26] Zhou B, Mi S, Mo X, Shih J, Tsai J, Hu E, Hsu M, Kay K, Yen Y. Time and sequence dependence of hydroxyurea in combination with Gemcitabine in human KB cells. Anticancer Res 2002;22:1369–77.
[27] Manni I, Mazzaro G, Gurtner A, Matovani R, Haugwitz U, Krause K, England K, Sacchi A, Soddu S, Piaggio G. NF-Y mediates the transcriptional inhibition of the cyclin B1, cyclin B2, and cdc25C promoter upon induced G2 arrest. J Biol Chem 2001;276:5570–6.
[28] Jung CP, Motwani MV, Schwartz GK. Flavopiridol increases sensitization to Gemcitabine in human gastrointestinal cancer cell lines and correlates with down-regulation of ribonucleotide reductase M2 subunit. Clin Cancer Res 2000;17:2527–36.
[29] Wong SJ, Myette MS, Wereley JP, Chitambar CR. Increased sensitivity of hydroxyurea-resistant leukemic cells to Gemcitabine. Clin Cancer Res 1999;5:439–43.
[30] Yen Y, Grill SP, Dutschman GE, Chang CN, Zhou BS, Cheng YC. Characterization of a hydroxyurea-resistant human KB cell line with supersensitivity to 6-thioguanine. Cancer Res 1994;54:3686–91.
[31] Zhou BS, Hsu NY, Pan BC, Doroshow JH, Yen Y. Overexpression of ribonucleotide reductase in transfected human KB cells increases their resistance to hydroxyurea: M2 but not M1 is sufficient to increase resistance to hydroxyurea in transfected cells. Cancer Res 1995;55: 1328–33.
[32] Mantovani R. A survey of 178 NF-Y binding CCAAT boxes. Nucleic Acids Res 1998;26:1135–43.
[33] Currie RA. NF-Y is associated with the histone acetyltransferases GCN5 and P/CAF. J Biol Chem 1998;273:1430–4.

[34] Huang A, Fan H, Taylor WR, Wright JA. Ribonucleotide reductase R2 gene expression and changes in drug sensitivity and genome stability. Cancer Res 1997;57:4876–81.

[35] Zhou BS, Tsai P, Ker R, Tsai J, Ho R, Yu J, Shih J, Yen Y. Overexpression of transfected human ribonucleotide reductase M2 subunit in human cancer cells enhances their invasive potential. Clin Exp Metastasis 1998;16:43–9.

[36] Amara FM, Chen FY, Wright JA. A novel transforming growth factor-β 1 responsive cytoplasmic trans-acting factor binds selectively to the 3′-untranslated region of mammalian ribonucleotide reductase R2 mRNA: role in message stability. Nucleic Acids Res 1993;21: 4803–9.

[37] Burton TR, Kashour T, Wright JA, Amara FM. Cellular signaling pathways affect the function of ribonucleotide reductase mRNA binding proteins: mRNA stabilization, drug resistance, and malignancy (Review). Int J Oncol 2003;22(1):21–31.

[38] Park SH, Lee SR, Kim BC, Cho EA, Patel SP, Kang HB, Sausville EA, Nakanishi O, Trepel JB, Lee BI, Kim SJ. Transcriptional regulation of the transforming growth factor β type II receptor gene by histone acetyltransferase and deacetylase is mediated by NF-Y in human breast cancer cells. J Biol Chem 2002;277:5168–74.

[39] Caretti G, Salsi V, Vecchi C, Imbriano C, Mantovani R. Dynamic recruitment of NF-Y and histone acetyltransferases on cell-cycle promoters. J Biol Chem 2003;278:30435–40.